

Discovery of the First M₅-Selective and CNS Penetrant Negative Allosteric Modulator (NAM) of a Muscarinic Acetylcholine Receptor: (S)-9b-(4-Chlorophenyl)-1-(3,4-difluorobenzoyl)-2,3-dihydro-1*H*-imidazo[2,1-*a*]isoindol-5(9*bH*)-one (ML375)

Patrick R. Gentry,^{†,‡,§} Masaya Kokubo,^{†,‡,§} Thomas M. Bridges,^{†,‡,§} Nathan R. Kett,^{†,‡,§} Joel M. Harp,^{||} Hyekyung P. Cho,^{†,‡,§} Emery Smith,[¶] Peter Chase,[¶] Peter S. Hodder,[¶] Colleen M. Niswender,^{†,‡,§} J. Scott Daniels,^{†,‡,§} P. Jeffrey Conn,^{†,‡,§} Michael R. Wood,^{†,‡,⊥,§} and Craig W. Lindsley^{*,†,‡,⊥,§}

[†]Department of Pharmacology, [‡]Vanderbilt Center for Neuroscience Drug Discovery, and [§]Vanderbilt Specialized Chemistry Center for Accelerated Probe Development (MLPCN), Vanderbilt University Medical Center, Nashville, Tennessee 37232, United States

^{||}Department of Biochemistry and [⊥]Department of Chemistry, Vanderbilt University, Nashville, Tennessee 37232, United States

[¶]Lead Identification Division, Translational Research Institute, Scripps Research Institute Molecular Screening Center, 130 Scripps Way, Jupiter, Florida 33458, United States

Supporting Information

ABSTRACT: A functional high throughput screen and subsequent multidimensional, iterative parallel synthesis effort identified the first muscarinic acetylcholine receptor (mAChR) negative allosteric modulator (NAM) selective for the M₅ subtype. ML375 is a highly selective M₅ NAM with submicromolar potency (human M₅ IC₅₀ = 300 nM, rat M₅ IC₅₀ = 790 nM, M₁–M₄ IC₅₀ > 30 μM), excellent multispecies PK, high CNS penetration, and enantiospecific inhibition.

■ INTRODUCTION

The five G-protein-coupled muscarinic acetylcholine receptors (mAChRs or M₁–M₅) utilize acetylcholine as their endogenous agonist and are broadly distributed throughout the periphery and central nervous system (CNS) where they regulate a diverse array of physiological processes.^{1–4} M₁ and M₄ are predominantly expressed within the CNS and have the highest expression levels. M₂ and M₃ are expressed in the periphery and moderately within the CNS, while M₅ expression is low (<2% of the total CNS mAChR population).^{2,5} Localization studies have found low levels of M₅ expression in multiple brain regions, but M₅ mRNA is the only mAChR transcript identified in dopaminergic neurons of the substantia nigra pars compacta (SNc) and ventral tegmental area (VTA).^{4–7} Here, M₅ is coexpressed with D₂ dopamine mRNA, which has led to the hypothesis that M₅ might modulate dopaminergic neurotransmission and function in addiction/reward mechanisms.⁶ Subsequent studies in M₅^{−/−} mice confirmed this hypothesis, with M₅^{−/−} mice showing reduced morphine and cocaine-conditioned place preference and self-administration, with no effect on food intake, suggesting preferential abuse-related effects.^{8–10} Thus, much of our current understanding of the function of M₅ has come from M₅ receptor localization, M₅^{−/−} mice, and experiments conducted with nonselective, orthosteric muscarinic ligands, as no M₅-selective antagonists or negative allosteric modulators (NAMs) have been reported.⁴ Recently, targeting allosteric sites on mAChRs has led to the discovery of highly selective positive allosteric modulators (PAMs) of M₁, M₄, and M₅,^{11–16} however, highly selective NAMs for individual subtypes have not yet been identified for any of the five mAChRs, and only one M₁-selective orthosteric

antagonist chemotype has been reported.¹⁷ Therefore, to address this limitation in small molecule tools to study M₅ function, we elected to pursue the discovery and development of selective M₅ NAMs to enable the dissection of the physiological role and therapeutic potential of M₅ inhibition.

■ RESULTS AND DISCUSSION

High-Throughput Screen. We performed a triple-add, functional high-throughput screen to identify M₅ modulator leads.^{16,18} For this effort, we screened the MLPCN¹⁹ collection (360 000 compounds) in Chinese hamster ovary (CHO) cells stably expressing human M₅ (hM₅) and measuring intracellular calcium mobilization. This effort identified 3920 M₅ primary hits (1.07% hit rate). Counterscreening against the parental CHO cell line and CHO cells expressing human M₁ and human M₄ and reconfirmation of powders in 10-point concentration–response curves (CRCs) resulted in nine confirmed, selective antagonists of hM₅.²⁰ At this point, it was not clear if these confirmed hits were selective M₅ orthosteric antagonists or negative allosteric modulators (NAMs).

Chemistry. Of the confirmed hits (Figure 1), our attention focused on **1**, a unique 2,3-dihydro-1*H*-imidazo[2,1-*a*]isoindol-5(9*bH*)-one-based scaffold, which was inactive on M₁ and M₄ but displayed weak inhibition of M₅ (IC₅₀ > 10 μM, 41% ACh Min). Upon a simple two-step resynthesis involving condensation of ethylene diamine and 2-benzoylbenzoic acid **2** to provide **3** and subsequent acylation (Scheme 1), we were pleased to observe enhanced activity of fresh powder of **1** at M₅

Received: August 28, 2013



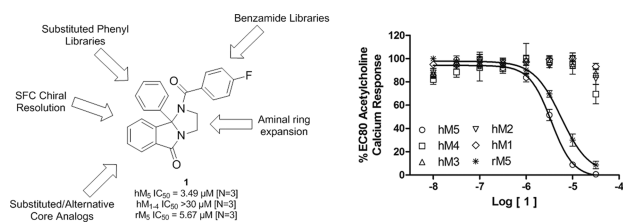
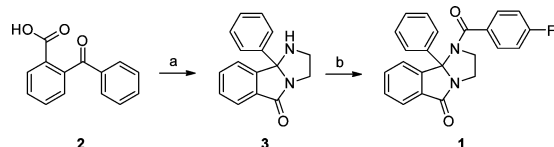


Figure 1. Structure, pharmacology (hM_5 IC_{50} = 3.49 μ M, rM_5 IC_{50} = 5.67 μ M, M_1 – M_4 IC_{50} > 30 μ M), and chemical optimization plan for **1**.

Scheme 1. Synthesis of **1** and Route for Analogue Synthesis^a



^aReagents and conditions: (a) ethylenediamine, *p*-TSA, toluene, reflux, Dean–Stark trap, 80%; (b) 4-fluorobenzoyl chloride, DCM, DIPEA, 93%.

(hM_5 IC_{50} = 3.49 μ M, rM_5 IC_{50} = 5.67 μ M) and no activity at the other four mAChRs (hM_1 – M_4 IC_{50} > 30 μ M).²⁰ Figure 1 also highlights the chemical optimization strategy for **1**, evaluating multiple dimensions simultaneously through iterative parallel synthesis, necessitated by the often shallow nature of allosteric SAR.¹¹

The first round of library synthesis evaluated alternate amides; thus, **3** was subsequently acylated with an array of 40 acid chlorides (aryl, heteroaryl, and aliphatic) according to Scheme 1 to provide analogues **4**. The library was efficiently triaged in a 10 μ M single point assay against an EC_{80} of ACh on human M_5 .¹⁵ SAR was shallow, with only seven analogues significantly reducing the EC_{80} , and only benzamide congeners were active. As shown in Table 1, a 3,4-difluoro analogue, **4g**, proved to be the most active (hM_5 IC_{50} = 1.0 μ M, rM_5 IC_{50} = 2.1 μ M), and it also maintained excellent mAChR selectivity (M_1 – M_4 IC_{50} > 30 μ M).

Other library efforts led exclusively to inactive analogues.²⁰ Expansion of the aminor ring to a six-membered congener was inactive. Conversion of the isoindolinone core to an azaindolinone proved to be inactive, as did urea, sulfonamide, and tertiary amine derivatives as replacements for the amide

Table 1. Structures and activities of analogs **4**

Entry	R			
		hM_5 pIC_{50} ^a	hM_5 IC_{50} (μ M)	ACh Min ^a (%)
4a	4-OCF ₃	5.35 \pm 0.03	4.47	0.2 \pm 2.4
4b	4-SCF ₃	5.86 \pm 0.02	1.38	0.5 \pm 1.5
4c	4-CF ₃	5.71 \pm 0.03	1.95	-2.4 \pm 1.4
4d	3-CF ₃	5.52 \pm 0.06	3.02	-0.7 \pm 5.2
4e	3,5-diCl	5.24 \pm 0.17	5.75	0.0 \pm 18.9
4f	3,5-diF	5.42 \pm 0.06	3.80	-2.2 \pm 5.6
4g	3,4-diF	5.98 \pm 0.02	1.05	0.0 \pm 1.3

^a(*) hM_5 pIC_{50} and ACh Min data reported as averages \pm SEM from our calcium mobilization assay; n = 3.

linkage. These data suggested that both the 2,3-dihydro-1*H*-imidazo[2,1-*a*]isoindol-5(9*bH*)-one core and the benzamide moiety were critical for M_5 activity.

Our attention then focused on introducing substituents into the 9*b* phenyl ring of **1** and assessing the impact on M_5 activity. Once again, analogues **5**–**7** were prepared following Scheme 1 but employing functionalized congeners of **2** in a matrix library (3 \times 10). As shown in Table 2, SAR was shallow and

Table 2. Structures and Activities of Analogues **5**–**7**^a

Entry	R ₁	R ₂			
			hM_5 pIC_{50}	hM_5 IC_{50} (μ M)	ACh Min ^a (%)
5a	Cl	4-OCF ₃	5.63 \pm 0.06	2.3	-5.3 \pm 4.4
5b		4-SCF ₃	5.52 \pm 0.13	3.0	-9.2 \pm 8.7
5c		4-CF ₃	5.69 \pm 0.04	2.0	0.7 \pm 2.3
5d		3-CF ₃	5.31 \pm 0.11	4.9	-7.2 \pm 8.0
5e		4-Me	5.58 \pm 0.04	2.6	0.1 \pm 2.8
5f	F	3,5-diF	6.00 \pm 0.04	1.0	2.8 \pm 2.0
5g		3,4-diF	6.32 \pm 0.02	0.48	0.1 \pm 1.0
6a		4-OCF ₃	---	>10	---
6b		4-SCF ₃	5.89 \pm 0.03	1.3	-0.2 \pm 1.7
6c		4-CF ₃	---	>10	---
6d	Me	3-CF ₃	5.68 \pm 0.03	2.1	-2.4 \pm 1.8
6e		4-Me	---	>10	---
6f		3,5-diF	---	>10	---
6g		3,4-diF	---	>10	---
7a		4-OCF ₃	5.46 \pm 0.06	3.5	-0.2 \pm 4.3
7b		4-SCF ₃	5.39 \pm 0.08	4.1	4.1 \pm 5.5
7c		4-CF ₃	---	>10	---
7d		3-CF ₃	---	>10	---
7e		4-Me	---	>10	---
7f		3,5-diF	5.63 \pm 0.05	2.3	-1.1 \pm 3.3
7g		3,4-diF	5.58 \pm 0.06	2.6	-6.8 \pm 4.3

^a(*) hM_5 pIC_{50} and ACh Min data reported as averages \pm SEM from our calcium mobilization assay; n = 3; ---, not determined.

unpredictable, with the data suggesting a cooperative relationship between benzamide and 9*b* phenyl substituents. However, one analogue, **5g**, possessing the 3,4-difluorobenzamide and a 9*b* 4-chlorophenyl moiety, afforded submicromolar potency at M_5 (hM_5 IC_{50} = 0.48 μ M, rM_5 IC_{50} = 1.1 μ M) and no activity at the other four mAChRs (hM_1 – M_4 IC_{50} > 30 μ M). This was an exciting result, as this was the racemic form of the analogue with potential for enantioselective inhibition of M_5 .²⁰

We were able to quickly develop supercritical fluid chromatography (SFC) conditions to separate the pure enantiomers of **5g** to provide **8** and **9**, both in >99% ee.²⁰ Optical rotations were recorded, and the (–)-enantiomer **8** proved to be active (hM_5 IC_{50} = 300 nM), whereas the (+)-enantiomer **9** was devoid of M_5 activity (hM_5 IC_{50} > 30 μ M) as shown in Figure 2. However, the absolute stereochemistry was unknown. Ultimately, single X-ray crystallography indicated that the active (–)-enantiomer **8** possessed the (*S*)-stereochemistry. Thus, this core showed enantiospecific activity for the inhibition of M_5 .

Molecular Pharmacology. The SAR was driven using a human M_5 functional assay, and since we desired an in vivo tool compound, we also evaluated **8** against rat M_5 . There was a slight species difference, with **8** displaying a >2-fold loss in activity at the rat M_5 receptor (rM_5 IC_{50} = 790 nM). However, **8** was inactive at human M_1 – M_4 (Figure 3A) and rat M_1 – M_4 (Figure 3B), representing the first M_5 selective small molecule inhibitor. To determine the mechanism of action of **8**, whether

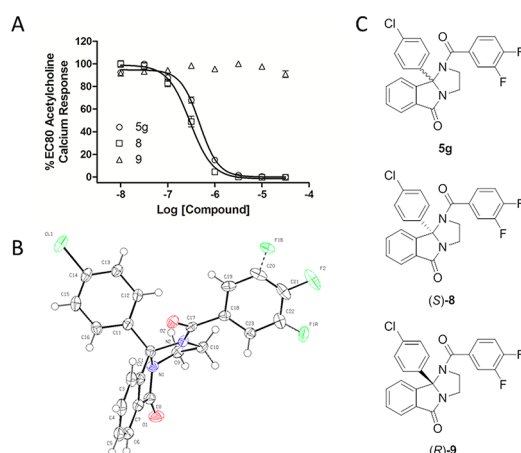


Figure 2. Structures and activities of the (S)- and (R)-enantiomers, **8** (hM_5 IC_{50} = 300 nM) and **9** (hM_5 IC_{50} > 30 μ M), respectively, of **5g** (hM_5 IC_{50} = 480 nM): (A) M_5 CRC for racemic **5g**, **8**, and **9**; (B) X-ray crystal structure of **8** (CCDC 953105); (C) structures of **5g**, **8**, and **9**.

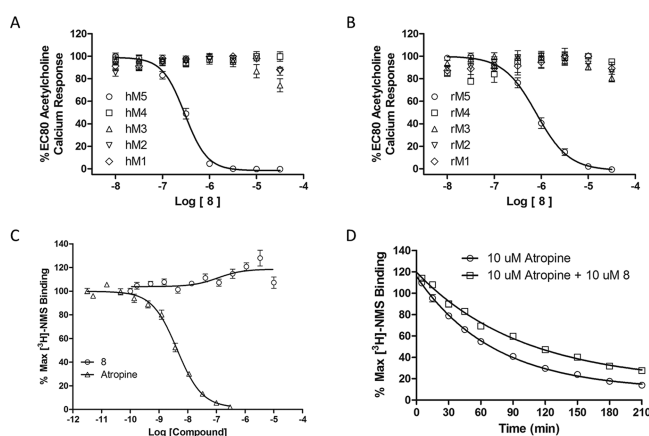


Figure 3. Molecular pharmacology profile of **8**: (A) human mAChR selectivity, where **8** is selective for hM_5 (hM_5 IC_{50} = 300 nM, hM_1 – M_4 IC_{50} > 30 μ M); (B) rat mAChR selectivity, where **8** is selective for rM_5 (rM_5 IC_{50} = 790 nM, rM_1 – M_4 IC_{50} > 30 μ M); (C) [3 H]NMS competition binding [N = 3] in membranes prepared from hM_5 cells. This strongly suggests that **8** does not bind at the M_5 orthosteric site. (D) [3 H]NMS dissociative kinetics [N = 3]. Atropine (alone) $t_{1/2}$ = 49.9 min, atropine (+**8**) $t_{1/2}$ = 68.8 min. **8** exerts an allosteric effect on the orthosteric site.

orthosteric or allosteric, we first performed competition binding experiments with the orthosteric mAChR antagonist [3 H]NMS and compared this to atropine. Compound **8** displayed no competition [3 H]NMS for binding to hM_5 , suggesting an

allosteric mode of receptor inhibition (Figure 3C).^{13–15,20} To further investigate an allosteric mechanism, we also performed [3 H]NMS dissociation kinetic experiments (Figure 3D), with hM_5 cell membranes, which revealed that **8** decreased the dissociation rate of [3 H]NMS, further confirming an allosteric effect of **8** on the orthosteric site.^{13–15,19} Thus, **8** is the first M_5 -selective negative allosteric modulator (NAM).

Metabolism and Disposition. Evaluation of the in vitro and in vivo DMPK profile^{20,21} of **8** (Table 3) revealed the compound to possess high metabolic stability with low hepatic microsomal intrinsic clearance (CL_{int} ; human, 2.6 mL min⁻¹ kg⁻¹; cynomolgus monkey (cyno), 20 mL min⁻¹ kg⁻¹; rat, 24 mL min⁻¹ kg⁻¹) and a corresponding low predicted hepatic clearance in multiple species (CL_{hep} ; human, 2.3 mL min⁻¹ kg⁻¹; cyno, 14 mL min⁻¹ kg⁻¹; rat, 18 mL min⁻¹ kg⁻¹). Correspondingly, **8** exhibited low clearance (CL_p , 2.5 mL min⁻¹ kg⁻¹) and a long elimination half-life ($t_{1/2}$, 80 h) in rodents (male, Sprague–Dawley rat, 1 mg/kg iv, n = 2) and non-human primates (male, cynomolgus monkey, 1 mg/kg, CL_p = 3.0 mL min⁻¹ kg⁻¹, $t_{1/2}$ = 10 h, n = 3). Consistent with a low clearance compound, **8** also demonstrated high oral bioavailability (F = 80%) following administration of a suspension-dose to male SD rats (n = 2) with a maximal plasma concentration (C_{max}) of 1.4 μ M and a corresponding time to reach C_{max} (T_{max}) of 7 h. The distribution of **8** was characterized by a low fraction unbound in plasma ($f_{u,p}$; human, 0.013; cyno, 0.001; rat, 0.029) and a high nonspecific binding in brain homogenate ($f_{u,br}$; rat, 0.003). Following an oral CNS distribution study in rat (male, Sprague–Dawley, n = 2; 10 mg/kg) we observed total and unbound brain-plasma partition coefficients of 1.8 and 0.2 (K_p and $K_{p,u}$, respectively) 1 h postadministration.

Compound **8** displayed an acceptable human cytochrome P450 inhibition profile producing acceptable IC_{50} for 3A4 (16 μ M), 1A2 (25 μ M, 2C9 (7.4 μ M), and 2D6 (26 μ M). Moreover, in a Eurofins radioligand binding panel of 68 GPCRs, ion channels, and transporter,²⁰ compound **8** displayed significant binding (>50% inhibition @10 μ M) at only one target (CB₁, 66%) but no functional activity at this target in a subsequent assay.

CONCLUSION

In summary, we have developed **8** (also referred to as ML375 or VU0483253), the first mAChR NAM that selectively targets M_5 (hM_5 IC_{50} = 300 nM, hM_1 – M_4 IC_{50} > 30 μ M), with a favorable DMPK profile and CNS penetration. Enantiospecific M_5 activity was noted, with all activity residing in the (S)-enantiomer, **8**. Because of the unexpected human–rodent species difference in regard to M_5 potency and brain homogenate binding, **8** is not suitable for in vivo work in rodents but may achieve sufficient exposure in non-human

Table 3. DMPK Profile of **8**

parameter/species	rat (male, Sprague–Dawley)	NHP (male, cynomolgus)	human
hepatic microsome CL_{int} (mL/min/kg)	24	20	2.6
predicted CL_{hep}	18	14	2.3
f_u plasma, f_u brain	0.029, 0.003	0.001, –	0.013, –
CYP inhibition (P450, IC_{50})	–	–	3A4, 2D6, 1A2: >15; 2C9: 7.4
CL_p (mL/min/kg), elimination $t_{1/2}$ (h)	2.5, 80	3.0, 10	–
VD_{ss} (IV)	16 L/kg	1.9 L/kg	–
%F (PO)	80	–	–
brain–plasma K_p , $K_{p,u}$ (1.0 h, PO)	1.8, 0.2	–	–

primate. Current efforts are focused on a new optimization program, driving the SAR on rat M₅ to deliver an in vivo tool for rodent addiction studies, and progress will be reported in due course.

EXPERIMENTAL SECTION

Chemistry. The general chemistry, experimental information, and syntheses of all other compounds are in the Supporting Information.

(S)-9b-(4-Chlorophenyl)-1-(3,4-difluorobenzoyl)-2,3-dihydro-1H-imidazo[2,1-*a*]isoindol-5(9bH)-one (8). To a mixture of 2-(4-chlorobenzoyl)benzoic acid (5.21 g, 20.0 mmol, 1 equiv) and ethylenediamine (2.67 mL, 40.0 mmol, 2 equiv) in toluene (30 mL, 0.67 M) was added *p*-toluenesulfonic acid monohydrate (~0.1 g, 3 mol %). A Dean–Stark trap was used to remove water, while the mixture was allowed to stir at reflux for 4 h. After cooling to ambient temperature, the mixture was dissolved in dichloromethane. The organic layer was washed with a saturated aqueous solution of sodium bicarbonate and then with brine. Solvent was removed under reduced pressure and the crude product was recrystallized from ethanol to give 2.86 g of pure 9b-(4-chlorophenyl)-2,3-dihydro-1H-imidazo[2,1-*a*]isoindol-5(9bH)-one (50.2% yield). To a solution of 9b-(4-chlorophenyl)-2,3-dihydro-1H-imidazo[2,1-*a*]isoindol-5(9bH)-one (15 mg, 0.053 mmol, 1.0 equiv) and DIPEA (18 μ L, 0.105 mmol, 2.0 equiv) in DCM (0.53 mL, 0.1 M) was added 3,4-difluorobenzoyl chloride (9.9 μ L, 0.079 mmol, 1.5 equiv). The mixture was allowed to stir at ambient temperature for 2 h. The reaction was quenched with methanol, and the organics were concentrated on a heated air-drying block. Crude product was purified via Gilson preparative LC to obtain 12.0 mg of **5g** (53.3% yield). The second eluting pure enantiomer of **5g** was separated via CO₂ supercritical fluid chromatography (Lux cellulose-3, 10 mm \times 250 mm column at 40 $^{\circ}$ C, back-pressure regulated at 100 bar, MeOH cosolvent, 10% isocratic prep over 7 min at 15 mL/min) and was determined to have >98% ee by chiral HPLC analysis (Lux cellulose-3, 4.6 mm \times 250 mm column at 40 $^{\circ}$ C, back-pressure regulated at 100 bar, MeOH cosolvent, 5–50% over 7 min at 3.5 mL/min). ¹H NMR (400.1 MHz, CDCl₃) δ (ppm): 8.04–7.99 (m, 1H); 7.90–7.85 (m, 1H); 7.65–7.56 (m, 2H); 7.38–7.30 (m, 3H); 7.25–7.19 (m, 2H); 7.18–7.14 (m, 2H); 4.38–4.30 (m, 1H); 4.01–3.93 (m, 1H); 3.82–3.75 (m, 1H); 3.34–3.25 (m, 1H). ¹³C NMR (100.6 MHz, CDCl₃) δ (ppm): 172.07, 166.84, 151.81 (dd, *J*_{C–F} = 254 Hz, 12.7 Hz), 150.33 (dd, *J*_{C–F} = 252 Hz, 13 Hz) 145.77, 136.65, 134.94, 133.55, 132.91 (t, *J* = 4.8 Hz), 131.88, 130.61, 129.06, 128.97, 127.53, 124.03, 123.62 (dd, *J* = 6.8 Hz, 4 Hz), 117.94 (d, *J* = 17 Hz), 116.83 (d, *J* = 18 Hz), 87.37, 52.24, 39.70. SFC (214 nM) *t*_R = 3.591 min (>98%). HRMS (TOF, ES⁺) C₂₃H₁₆N₂O₂F₂Cl [M + H]⁺ calcd mass 425.0868, found 425.0872. Specific rotation [α]_D²³ –168.6 $^{\circ}$ (c 0.75, CHCl₃).

ASSOCIATED CONTENT

Supporting Information

Experimental procedures and spectroscopic data for selected compounds, detailed pharmacology, and DMPK methods. This material is available free of charge via the Internet at <http://pubs.acs.org>.

AUTHOR INFORMATION

Corresponding Author

*Phone: 615-322-8700. Fax: 615-343-3088. E-mail: craig.lindsley@vanderbilt.edu.

Notes

The authors declare no competing financial interest.

ACKNOWLEDGMENTS

This work was generously supported by the NIH/MLPCN Grant U54 MH084659 (C.W.L.) and Grant U54 MH084512 (Scripps).

ABBREVIATIONS USED

M₅, muscarinic acetylcholine receptor subtype 5; CRC, concentration–response curve; NAM, negative allosteric modulator; MLPCN, Molecular Libraries Probe Production Centers Network

REFERENCES

- (1) Smythies, J. Section I. The cholinergic system. *Int. Rev. Neurobiol.* **2005**, *64*, 1–122.
- (2) Wess, J.; Eglen, R. M.; Gautam, D. Muscarinic acetylcholine receptors: mutant mice provide new insights for drug development. *Nat. Rev. Drug Discovery* **2007**, *6*, 721–733.
- (3) Langmead, C. J.; Watson, J.; Reavill, C. Muscarinic acetylcholine receptors as drug targets. *Pharmacol. Ther.* **2008**, *117*, 232–243.
- (4) Denker, D.; Thomsen, M.; Wortwein, G.; Weikop, G.; Cui, Y.; Jeon, J.; Wess, J.; Fink-Jensen, A. Muscarinic acetylcholine receptor subtypes as potential drug targets for the treatment of schizophrenia, drug abuse and Parkinson's disease. *ACS Chem. Neurosci.* **2012**, *3*, 80–89.
- (5) Caulfield, M. P.; Birdsall, N. J. M. Classification of muscarinic acetylcholine receptors. *Pharmacol. Rev.* **1998**, *50*, 279–290.
- (6) Weiner, D. M.; Levey, A. I.; Brann, M. R. Expression of muscarinic acetylcholine and dopamine receptor messenger-RNAs in rat basal ganglia. *Proc. Natl. Acad. Sci. U.S.A.* **1990**, *87*, 7050–7054.
- (7) Yasuda, R. P.; Ciesla, W.; Flores, L. R.; Wall, S. J.; Li, M.; Satkus, S. A.; Weissstein, J. S.; Spagnola, B. V.; Wolfe, B. B. Development of antisera selective for M4 and M5 muscarinic cholinergic receptors—distribution of M4 and M5 receptors in rat-brain. *Mol. Pharmacol.* **1993**, *43*, 149–157.
- (8) Basile, A. S.; Fedorova, I.; Zapata, A.; Liu, X.; Shippenberg, T.; Duttaray, A.; Yamada, M.; Wess, J. Deletion of the M5 muscarinic acetylcholine receptor attenuates morphine reinforcement and withdrawal but not morphine analgesia. *Proc. Natl. Acad. Sci. U.S.A.* **2002**, *99*, 11452–11457.
- (9) Fink-Jensen, A.; Fedorova, I.; Wörtwein, G.; Woldbye, D. P.; Rasmussen, T.; Thomsen, M.; Bolwig, T. G.; Knitowski, K. M.; McKinzie, D. L.; Yamada, M.; Wess, J.; Basile, A. Role for M5 muscarinic acetylcholine receptors in cocaine addiction. *J. Neurosci. Res.* **2003**, *74*, 91–96.
- (10) Thomsen, M.; Woldbye, D. P.; Wortwein, G.; Fink-Jensen, A.; Wess, J.; Caine, S. B. Reduced cocaine self-administration in muscarinic M5 acetylcholine receptor-deficient mice. *J. Neurosci.* **2005**, *25*, 8141–8149.
- (11) Melancon, B. J.; Hopkins, C. R.; Wood, M. R.; Emmitte, K. A.; Niswender, C. M.; Christopoulos, A.; Conn, P. J.; Lindsley, C. W. Allosteric modulation of 7 transmembrane spanning receptors: theory, practice and opportunities for CNS drug discovery. *J. Med. Chem.* **2012**, *55*, 1445–1464.
- (12) Conn, P. J.; Jones, C.; Lindsley, C. W. Subtype selective allosteric modulators of muscarinic receptors for the treatment of CNS disorders. *Trends Pharmacol. Sci.* **2009**, *30*, 148–156.
- (13) Tarr, J. C.; Turlington, M. L.; Reid, P. R.; Utely, T. J.; Sheffler, D. J.; Cho, H. P.; Klar, R.; Pancani, T.; Klein, M. T.; Bridges, T. M.; Morrison, R. D.; Xiang, Z.; Daniels, S. J.; Niswender, C. M.; Conn, P. J.; Wood, M. R.; Lindsley, C. W. Targeting selective activation of M₁ for the treatment of Alzheimer's disease: further chemical optimization and pharmacological characterization of the M₁ positive allosteric modulators ML169. *ACS Chem. Neurosci.* **2012**, *3*, 884–895.
- (14) Brady, A.; Jones, C. K.; Bridges, T. M.; Kennedy, P. J.; Thompson, A. D.; Breining, M. L.; Gentry, P. R.; Yin, H.; Jadhav, S. B.; Shirey, J.; Conn, P. J.; Lindsley, C. W. Centrally active allosteric potentiators of the M₄ muscarinic acetylcholine receptor reverse amphetamine-induced hyperlocomotion behavior in rats. *J. Pharmacol. Exp. Ther.* **2008**, *327*, 941–953.
- (15) Bridges, T. M.; Marlo, J. E.; Niswender, C. M.; Jones, J. K.; Jadhav, S. B.; Gentry, P. R.; Weaver, C. D.; Conn, P. J.; Lindsley, C. W. Discovery of the first highly M₅-preferring muscarinic acetylcholine receptor ligand, an M₅ positive allosteric modulator derived from a

series of 5-trifluoromethoxy *N*-benzyl isatins. *J. Med. Chem.* **2009**, *52*, 3445–3448.

(16) Gentry, P. R.; Bridges, T. M.; Lamsal, A.; Vinson, P. N.; Smith, E.; Chase, P.; Hodder, P. S.; Engers, J. L.; Niswender, C. M.; Daniels, J. S.; Conn, P. J.; Wood, M. R.; Lindsley, C. W. Discovery of ML326: the first sub-micromolar, selective M₅ PAM. *Bioorg. Med. Chem. Lett.* **2013**, *23*, 2996–3000.

(17) Sheffler, D. J.; Williams, R.; Bridges, T. M.; Lewis, L. M.; Xiang, Z.; Zheng, F.; Kane, A. S.; Byum, N. E.; Jadhav, S.; Mock, M. M.; Zheng, F.; Lewis, L. M.; Jones, C. K.; Niswender, C. M.; Weaver, C. D.; Conn, P. J.; Lindsley, C. W.; Conn, P. J. Novel selective muscarinic acetylcholine receptor subtype 1 (M₁ mAChR) antagonist reduces seizures without impairing hippocampal-dependent learning. *Mol. Pharmacol.* **2009**, *76*, 356–368.

(18) Marlo, J. E.; Niswender, C. M.; Luo, Q.; Brady, A. E.; Shirey, J. K.; Rodriguez, A. L.; Bridges, T. M.; Williams, R.; Days, E.; Nalywajko, N. T.; Austin, C.; Williams, M.; Xiang, Y.; Orton, D.; Brown, H. A.; Kim, K.; Lindsley, C. W.; Weaver, C. D.; Conn, P. J. Discovery and characterization of novel allosteric potentiators of M₁ muscarinic receptors reveals multiple modes of activity. *Mol. Pharmacol.* **2009**, *75*, 577–588.

(19) For the MLPCN see <http://mli.nih.gov/mli/mlpcn/>. ML375 is an MLPCN probe and freely available upon request.

(20) See Supporting Information for full details.

(21) Wenthur, C. J.; Niswender, C. M.; Morrison, R.; Daniels, J. S.; Conn, P. J.; Lindsley, C. W. Discovery of (*R*)-(2-fluoro-4-((4-methoxyphenyl)ethynyl)phenyl)(3-hydroxypiperidin-1-yl)methanone (ML337), an mGlu₃ selective and CNS penetrant negative allosteric modulator (NAM). *J. Med. Chem.* **2013**, *56*, 3713–3718.